A theoretical study of exciton energy levels in laterally coupled quantum dots

2009 J. Phys.: Condens. Matter 21 405801

(http://iopscience.iop.org/0953-8984/21/40/405801)

J. Phys.: Condens. Matter **21** (2009) 405801 (8pp) doi:10.1088/0953-8984/21/40/405801

A theoretical study of exciton energy levels in laterally coupled quantum dots

Z Barticevic[1], M Pacheco[1], C A Duque[2] and L E Oliveira[3,4]

[1] Departamento de Física, Universidad Técnica Federico Santa María, Casilla 110-V, Valparaíso, Chile
[2] Instituto de Física, Universidad de Antioquia, AA 1226 Medellín, Colombia
[3] Instituto de Física, UNICAMP, CP 6165, Campinas, São Paulo 13083-970, Brazil
[4] Inmetro, Campus de Xerém, Duque de Caxias, Rio de Janeiro 25250-020, Brazil

Received 6 May 2009, in final form 13 August 2009
Published 14 September 2009
Online at stacks.iop.org/JPhysCM/21/405801

Abstract
A theoretical study of the electronic and optical properties of laterally coupled quantum dots, under applied magnetic fields perpendicular to the plane of the dots, is presented. The exciton energy levels of such laterally coupled quantum-dot systems, together with the corresponding wavefunctions and eigenvalues, are obtained in the effective-mass approximation by using an extended variational approach in which the magnetoexciton states are simultaneously obtained. One achieves the expected limits of one single quantum dot, when the distance between the dots is zero, and of two uncoupled quantum dots, when the distance between the dots is large enough. Moreover, present calculations—with appropriate structural dimensions of the two-dot system—are shown to be in agreement with measurements in self-assembled laterally aligned GaAs quantum-dot pairs and naturally/accidentally occurring coupled quantum dots in GaAs/GaAlAs quantum wells.

1. Introduction

Semiconductor quantum dots (QDs) are man-made nanostructures in which the carriers, i.e. electrons and holes, are confined in all spatial directions. In that respect, therefore, such QDs are often referred to as 'artificial atoms' as they show typical atomic properties like discrete energy levels and shell structures. One of the differences with respect to natural atoms, however, is that, in such QD nanostructures, the number of electrons and/or holes is tunable and the characteristic lengths of the whole system, such as those corresponding to an external confinement potential, electron–electron interaction and applied magnetic field, for instance, may be of comparable size. Starting from QDs as a nanostructure, more developed and complex systems are conceivable and likely to have prospects in future device applications. A trivial example is the analogy of a two-atom molecule with a semiconductor nanostructure consisting of two coupled QDs.

Vertical and lateral quantum couplings in individual QD molecules and its manipulation using applied magnetic/electric fields have been demonstrated [1, 2]. Ortner *et al* [1] studied the fine structure of excitons in InAs/GaAs QDs via photoluminescence (PL) spectroscopy in magnetic fields up to 8 T and observed anticrossings and mixings of optically bright and dark states in InAs/GasAs vertically coupled QDs as functions of the applied magnetic field. Krenner *et al* [2] observed anticrossing of different excitonic transitions in coupled GaInAs QDs as the applied electric field is tuned. Moreover, by using near-field and time-resolved PL measurements, Neogi *et al* [3] studied the exciton localization in vertically and laterally coupled GaN/AlN QDs and observed that, in multiple-period GaN QDs, the exciton binding energy is six times larger as compared with the corresponding value for a single-period QD, whereas the exciton lifetime in single GaN QDs is a factor of about ten times the corresponding lifetime in multiple QDs. For applications, however, one would normally prefer choosing laterally coupled QDs as, in principle, the lateral geometry enables coupling in two dimensions and thus allows for a natural up-scaling to very large numbers of quantum gates across a semiconductor substrate. Furthermore, for individual lateral QD molecules the realization of reliable gating between the constituent QDs should be relatively straightforward when compared to the vertically coupled case, where gating, although feasible, is technically very demanding. Moreover, the lateral positioning of QDs and QD molecules has already been demonstrated by Schmidt *et al* [4] and Songmuang *et al* [5]. Also, self-assembled laterally coupled (In, Ga)As QDs have been

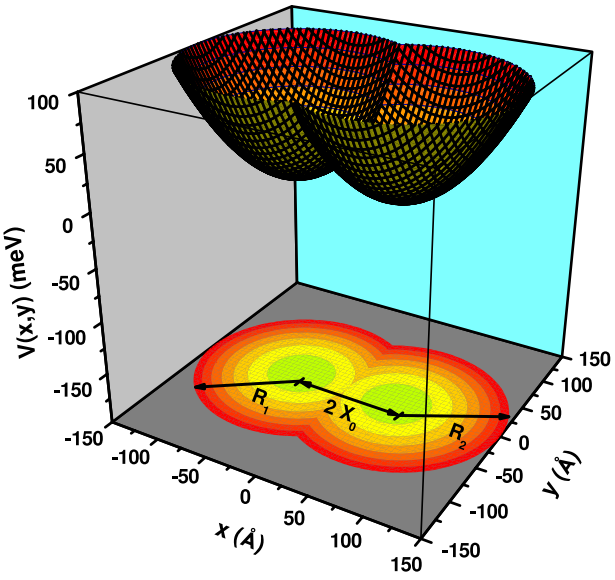

Figure 1. Pictorial view of the double-quantum-dot model potential used in the present work.

(This figure is in colour only in the electronic version)

observed by Beirne *et al* [6]. They demonstrated inter-dot electron coupling using optical techniques, with the degree of tunnel coupling controlled by applying a tunable static electric field along the QD molecule axis, a fact which may be used to create a wavelength-tunable single-photon emitter. Moreover, the fabrication of strain-free, laterally aligned GaAs–$Ga_{0.73}Al_{0.27}As$ QD pair structures was recently reported by Yamagiwa *et al* [7] by utilizing the droplet-epitaxy technique and the anisotropic surface potentials of the GaAs (100) surface for the migration of the Ga adatoms, with their PL measurements indicating the existence of tunnel coupling between the QDs. Kolb and Drew [8] performed a study of coupling in naturally/accidentally occurring GaAs QDs in GaAs/GaAlAs quantum wells. The QDs arise from monolayer fluctuations at the well interfaces of narrow 2 nm thick $Ga_{0.7}Al_{0.3}As$–GaAs–$Ga_{0.7}Al_{0.3}As$ quantum wells which lead to confinement in the growth plane. The possibility of the occurrence of naturally coupled QDs was examined by near-field scanning optical microscopy.

Motivated by the work by Yamagiwa *et al* [7] and Kolb and Drew [8], in the present work we are concerned with a theoretical study of confined magnetoexcitons in two laterally coupled QDs, under applied magnetic fields perpendicular to the plane of the dots. In order to describe the exciton wavefunction, we have followed the same procedure described in previous work [9, 10] in which the excitonic states have been obtained via an expansion of the exciton envelope wavefunctions in terms of products of hole and electron quantum-well states with appropriate Gaussian functions for the various excitonic states. The magnetoexcitonic transitions, together with the corresponding exciton wavefunctions and eigenvalues, are then obtained by using an extended variational approach in the effective-mass approximation in which the magnetoexciton states are simultaneously obtained.

This work is organized as follows. In section 2 we detail the present theoretical approach. Section 3 is concerned with the results and discussion and, finally, conclusions are given in section 4.

2. Theoretical framework

Here we are concerned with e–h correlated transition energies in two laterally coupled GaAs–$Ga_{1-x}Al_xAs$ QDs in the x–y plane, and consider the model Hamiltonian

$$H = H_e + H_h + V_{QD} + V_C, \tag{1}$$

where we take into account growth-direction-applied magnetic field effects, i.e. the electron and hole Hamiltonian operators are given as

$$H_e = -\frac{\hbar^2}{2m_e^*}\frac{\partial^2}{\partial z_e^2} + \frac{1}{2m_e^*}\left[-i\hbar(\nabla_e)_\parallel + \frac{e}{c}\overrightarrow{A}_e\right]^2, \tag{2}$$

and

$$H_h = -\frac{\hbar^2}{2m_{h_\perp}^*}\frac{\partial^2}{\partial z_h^2} + \frac{1}{2m_{h_\parallel}^*}\left[-i\hbar(\nabla_h)_\parallel - \frac{e}{c}\overrightarrow{A}_h\right]^2, \tag{3}$$

respectively, where m_e^* and m_h^* are the electron and hole effective masses. We note that in the present study we have considered a system of two coupled QDs in which the two dots have the same radius. Experimentally it is very difficult to reach such particular configurations. If the size of the two QDs is very different, the properties of the system will be dominated by the largest dot and an applied electric field would be necessary in order to couple the two QDs. However, if the sizes of the two QDs are similar, the system may be described as consisting of two identical QDs. The V_{QD} confinement potential of the double QD heterostructure is modeled by

$$V_{QD} = V_e(z_e) + V_h(z_h) + V(x, y), \tag{4}$$

i.e., a quantum-well potential has been considered for the confinement in the z direction, with $V_e(z_e) + V_h(z_h)$ corresponding to the sum of the electron and hole one-dimensional L square-well barrier potentials, x and y are the e–h in-plane coordinates, and the x–y in-plane $V(x, y)$ potential is taken as the superposition of parabolic potentials of each dot (cf figure 1), with their minima at different positions and truncated at the intersection plane in such a way that the carriers are confined in two well-defined regions of the x–y plane, named as QD regions, i.e.,

$$V(x, y) = \tfrac{1}{2}\mu_x\omega^2[(x - X_0)^2 + y^2]\Theta(x) + \tfrac{1}{2}\mu_x\omega^2[(x + X_0)^2 + y^2]\Theta(-x), \tag{5}$$

where

$$\mu_x = \frac{m_e^* m_{h_\parallel}^*}{m_e^* + m_{h_\parallel}^*} \tag{6}$$

is the heavy-hole exciton in-plane effective mass, $\Theta(x)$ is the Heaviside step function and $\hbar\omega$ is a measure of the strength of the in-plane confinement potential of each dot. The coupling or decoupling of the two dots is obtained by varying the $2X_0$

distance for which two limiting cases are obtained: (1) for $2X_0 = 0$ the electron–hole (e–h) pair is confined in a single QD and (2) for $2X_0 \to \infty$ the e–h pair is confined in either of two isolated QDs. It is convenient to define a lateral QD radius as

$$R_{\mathrm{QD}} = \sqrt{\frac{\hbar}{\mu_x\,\omega}}. \tag{7}$$

Alternatively, one may write $V(x, y)$ in the above equation as

$$V(\rho,\theta) = \tfrac{1}{2}\mu_x\omega^2\rho^2 - \mu_x\omega^2 X_0|\rho\cos(\theta)| + \tfrac{1}{2}\mu_x\omega^2 X_0^2, \tag{8}$$

where ρ and θ are the e–h in-plane coordinates. The e–h correlation is taken into account through

$$V_{\mathrm{C}} = -\frac{e^2}{\epsilon\sqrt{\rho^2 + (z_{\mathrm{e}} - z_{\mathrm{h}})^2}}, \tag{9}$$

i.e. a Coulomb potential screened by the dielectric constants of the barrier or well materials, where $r = \sqrt{\rho^2 + (z_{\mathrm{e}} - z_{\mathrm{h}})^2}$ is the e–h distance. In the above equations, the vector potential has been chosen in the symmetric gauge as

$$\vec{A} = \frac{B}{2}(-y, x, 0). \tag{10}$$

The z-dependent $V_i(z_i)$ ($i = \mathrm{e}, \mathrm{h}$) confinement potential is invariant under the transformation $z \to -z$. Therefore, one may assign a definite parity for the electron or hole quantum-well wavefunction. As the e–h Coulomb interaction is invariant under the simultaneous inversion of the electron and hole positions, the excitonic envelope wavefunction will therefore have a well-defined parity and the excitonic envelope function may be expanded as a product of quantum-well electron and hole eigenfunctions preserving the parity. As here we are studying the effects of the lateral confinement due to the two laterally coupled QDs, we work in the approximation in which the center of mass of the e–h pair is frozen and, therefore, the six-dimensional excitonic envelope wavefunction may be written as a four-dimensional one as

$$\Psi^{\pm}_{\mathrm{exc}}(\vec{\rho}, z_{\mathrm{e}}, z_{\mathrm{h}}) = \sum_{P,P'}\sum_{n_{\mathrm{e}}(P),n_{\mathrm{h}}(P')} B^{n_{\mathrm{e}}(P),n_{\mathrm{h}}(P'),(\pm)}(\vec{\rho})\, f_{n_{\mathrm{e}}(P)}(z_{\mathrm{e}})\, f_{n_{\mathrm{h}}(P')}(z_{\mathrm{h}})\, \triangle_{P,P'}, \tag{11}$$

where P and P' indicate even or odd parity, and $\triangle_{P,P'} = \delta_{P,P'}$ for even (+) excitonic states whereas $\triangle_{P,P'} = 1 - \delta_{P,P'}$ for odd (−) states. In the above, $f_{n_{\mathrm{e}}(P)}(z_{\mathrm{e}})$ and $f_{n_{\mathrm{h}}(P')}(z_{\mathrm{h}})$ are the quantum-well electron and hole eigensolutions, respectively. One, therefore, obtains the following eigenvalue equation for $B^{n_{\mathrm{e}}(P),n_{\mathrm{h}}(P),(+)}(\rho,\theta)$ (and a similar equation for the (−) solution):

$$\left[-\frac{\hbar^2}{2\mu_x}\nabla^2_\rho + \frac{eB}{2c}\left(\frac{1}{m^*_{\mathrm{e}}} - \frac{1}{m^*_{\mathrm{h}_\parallel}}\right)L_z - \varepsilon(n_{\mathrm{e}}(P), n_{\mathrm{h}}(P)) + U(\rho,\theta)\right] B^{n_{\mathrm{e}}(P),n_{\mathrm{h}}(P),(+)}(\rho,\theta) - \sum_{P'}\sum_{n'_{\mathrm{e}}(P'),n'_{\mathrm{h}}(P')} V^{n_{\mathrm{e}}(P),n_{\mathrm{h}}(P)}_{n'_{\mathrm{e}}(P'),n'_{\mathrm{h}}(P')}(\rho) \times B^{n'_{\mathrm{e}}(P'),n'_{\mathrm{h}}(P'),(+)}(\rho,\theta) = 0, \tag{12}$$

where

$$U(\rho,\theta) = V(\rho,\theta) + \tfrac{1}{8}\mu_x\omega_{\mathrm{c}}^2\rho^2 = \tfrac{1}{2}\mu_x\omega_{\mathrm{eff}}^2\rho^2 - \mu_x\omega^2 X_0|\rho\cos(\theta)| + \tfrac{1}{2}\mu_x\omega^2 X_0^2, \tag{13}$$

$$V^{n_{\mathrm{e}}(P),n_{\mathrm{h}}(P)}_{n'_{\mathrm{e}}(P'),n'_{\mathrm{h}}(P')}(\rho) = \langle f_{n_{\mathrm{e}}(P)}(z_{\mathrm{e}})\, f_{n_{\mathrm{h}}(P)}(z_{\mathrm{h}})|V_{\mathrm{C}}|f_{n'_{\mathrm{e}}(P')}(z_{\mathrm{e}})\, f_{n'_{\mathrm{h}}(P')}(z_{\mathrm{h}})\rangle, \tag{14}$$

$$\varepsilon(n_{\mathrm{e}}(P), n_{\mathrm{h}}(P)) = E_{\mathrm{exc}} - E_{\mathrm{e}} - E_{\mathrm{hh}} - E_{\mathrm{g}}, \tag{15}$$

E_{g} is the bulk GaAs energy gap, E_{e} (E_{hh}) is the first electron (heavy-hole) z direction quantum-well barrier potential confinement energy, E_{exc} denotes the excitonic PL peak energy (or correlated eh transition energy) and

$$\omega_{\mathrm{eff}} = \sqrt{\omega^2 + \tfrac{1}{4}\omega_{\mathrm{c}}^2}, \tag{16}$$

with $\omega_{\mathrm{c}} = \frac{eB}{\mu_x c}$. We note that the $U(\rho,\theta)$ potential does not have azimuthal symmetry and, therefore, the m quantum numbers associated with the z component of the angular momentum are not good quantum numbers for the present problem. Moreover, the lateral potential in equation (8) is invariant under the transformation $\theta \to \theta + \pi$. Therefore, $B^{n_{\mathrm{e}}(P),n_{\mathrm{h}}(P'),(+)}(\rho,\theta)$ should have definite parity ('gerade' g or 'ungerade' u) under the interchange $\theta \to \theta + \pi$. One may then expand the $B^{n_{\mathrm{e}}(P),n_{\mathrm{h}}(P'),(+)}(\rho,\theta)$ functions in terms of the eigenfunctions of the angular momentum L_z as

$$B^{n_{\mathrm{e}}(P),n_{\mathrm{h}}(P),(+),g}(\rho,\theta) = \sum_{m=\mathrm{even}} \exp(\mathrm{i}m\theta)\, F^{(+,m)}_{n_{\mathrm{e}}(P),n_{\mathrm{h}}(P)}(\rho), \tag{17}$$

or

$$B^{n_{\mathrm{e}}(P),n_{\mathrm{h}}(P),(+),u}(\rho,\theta) = \sum_{m=\mathrm{odd}} \exp(\mathrm{i}m\theta)\, F^{(+,m)}_{n_{\mathrm{e}}(P),n_{\mathrm{h}}(P)}(\rho). \tag{18}$$

One then obtains a set of coupled equations for $F^{(+,m)}_{n_{\mathrm{e}}(P),n_{\mathrm{h}}(P)}(\rho)$, which may be solved numerically by expanding $F^{(+,m)}$ in a set of Gaussian-type functions with length parameters λ, chosen in order to cover the physical range of relevant spatial parameters [9]. Further details of the calculation procedure may be found elsewhere [9, 10].

3. Results and discussion

In the following, we have considered the e–h Coulomb interaction as screened by the $\epsilon = 12.4$ static dielectric constant [11] of bulk GaAs throughout the heterostructure and image-charge effects have been ignored. For the electron and hole effective masses [11] we have used $m^*_{\mathrm{e}}/m_0 = 0.0665$, $m^*_{\mathrm{hh}_\perp}/m_0 = 0.34$ and $m^*_{\mathrm{hh}_\parallel}/m_0 = 0.116$.

Figures 2 and 3 present results for the exciton energy transitions in laterally coupled GaAs–$Ga_{1-x}Al_xAs$ double QDs with dimensions such that $R = 50$ Å (or $R = 150$ Å) for the radius of each dot and $L = 20$ Å for the quantum-well confinement in the growth direction. Calculations are performed without effects of the applied magnetic field. In the case of the lowest e–h transition (see figures 2(a) and 3(a)), the result for $X_0 = 0$ corresponds to the $m = 0$ ground-state e–h transition energy associated with an uncorrelated e–h pair confined in a single QD. As the $2X_0$ inter-dot distance

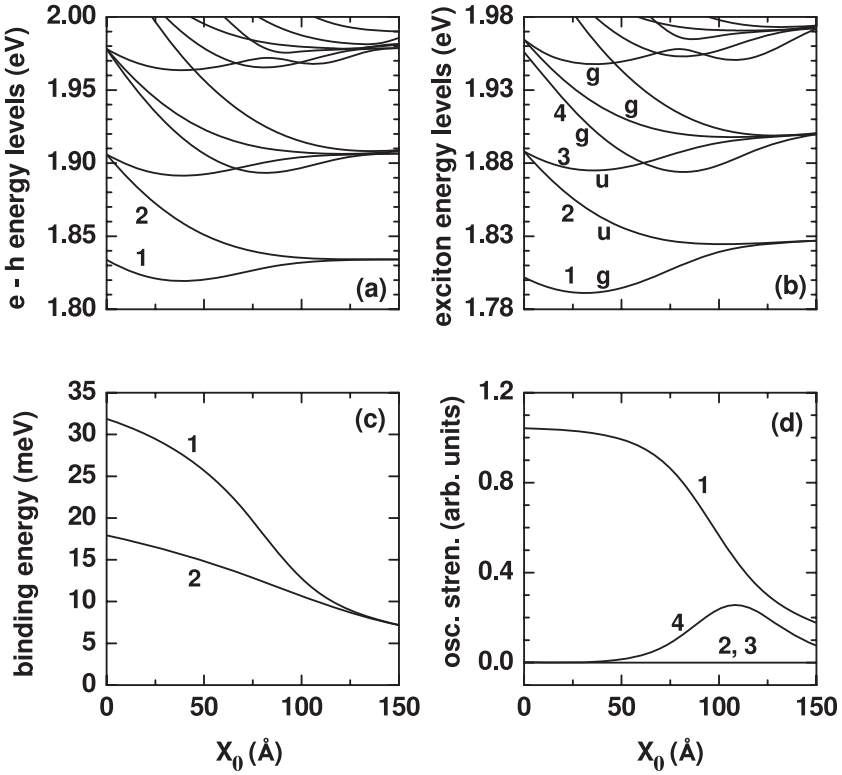

Figure 2. Non-correlated electron–heavy-hole (a) and corresponding exciton energy levels (b) for a laterally coupled GaAs–$Ga_{0.7}Al_{0.3}As$ double QD as a function of half of the distance between the centers of the two dots. The dimensions of the considered nanostructure are $R = 50$ Å for the radius of each dot and $L = 20$ Å for the quantum-well confinement along the growth direction. Results in (c) are for the exciton binding energy of the first two exciton states whereas in (d) the oscillator strength (light polarized in the x–y plane) is presented for the first four exciton peak energies. Labels g and u in (b) correspond to the symmetry associated with the lateral confinement (cf equations (17) and (18)). All depicted exciton energies in (b) correspond to states with even parity with respect to the z-confinement potential.

increases, one notices that the uncorrelated e–h transition energy decreases up to a minimum and then increases up to the value corresponding to two isolated QDs and one obtains a doubly degenerate $m = 0$ ground-state uncorrelated e–h transition energy, as expected. For $X_0 = 0$, at the energy of ≈1.906 eV (cf figure 2(a)), one obtains a doubly degenerate $m = -1$ and $+1$ transition energy, and as the $2X_0$ inter-dot distance increases, one recovers, for $X_0 = 150$ Å, a fourfold essentially degenerate transition energy at ≈1.91 eV associated with $m = -1$ and $+1$ uncorrelated e–h transitions in two isolated QDs. A similar discussion would apply to the calculated results shown in figure 3(a). With respect to the excitonic energy transitions (or correlated e–h transitions), calculated results may be interpreted as follows: for $X_0 = 0$, the exciton binding energy is ≈32 meV for the double-dot structure with dot radii equal to 50 Å (see figure 2), whereas it is ≈15 meV for dot radii equal to 150 Å (cf figure 3), i.e. a larger binding energy for smaller QD radius, as one would expect for the $X_0 = 0$ isolated single QD regime. On the other hand, the exciton binding energy is 7.2 meV for the double-dot nanostructure with $L = 20$ Å, $X_0 = 150$ Å and $R = 50$ Å (cf figure 2), whereas the correlated e–h pair has a binding energy of 6.5 meV for the coupled-dot structure with $L = 20$ Å, $X_0 = 300$ Å and $R = 150$ Å (cf figure 3). These results for somewhat large values of the $2X_0$ dot distance as compared to the dot radii indicate that, in both cases, effects of the Coulomb e–h interaction lead essentially to an exciton confined in a z direction $L = 20$ Å quantum well and a large-radius two-dimensional QD (here we just mention that the bulk GaAs exciton has a binding energy of ≈4 meV). The exciton binding energies for the first two exciton states are presented in figures 2(c) and 3(c). We note that, as the distance between the centers of the dots increases, the exciton binding energies decrease, as one would expect. Also note that the degeneracies are removed. In bulk GaAs the exciton binding energy for heavy-hole states is of the order of 4 meV and the Bohr radius 100 Å. Note that, for example in figure 2, the non-correlated electron and/or hole confined energies come from similar competition between the radial confinement, due to the parabolic potentials, and the confinement due to the square quantum wells. In the case of figure 3, the in-plane confinement is smaller than in the case of figure 2 as the radial dimensions of the quantum dots are of the order of the Bohr radius. We note that, for the 1s-like state in the 3D limit, the expectation value of the electron–hole distance is 1.5 effective Bohr radii, i.e. 150 Å. In the case of $L = 20$ Å, the energies for the electron and heavy-hole carriers due to the square quantum-well confinement are respectively 167 and 74 meV. For $R = 50$ Å, the energy associated with the in-plane confinement changes from 72 meV for both the strong or low coupling regimes to 69 meV in the intermediate coupling regime when the system behaves like an elliptical QD. For $R = 150$ Å,

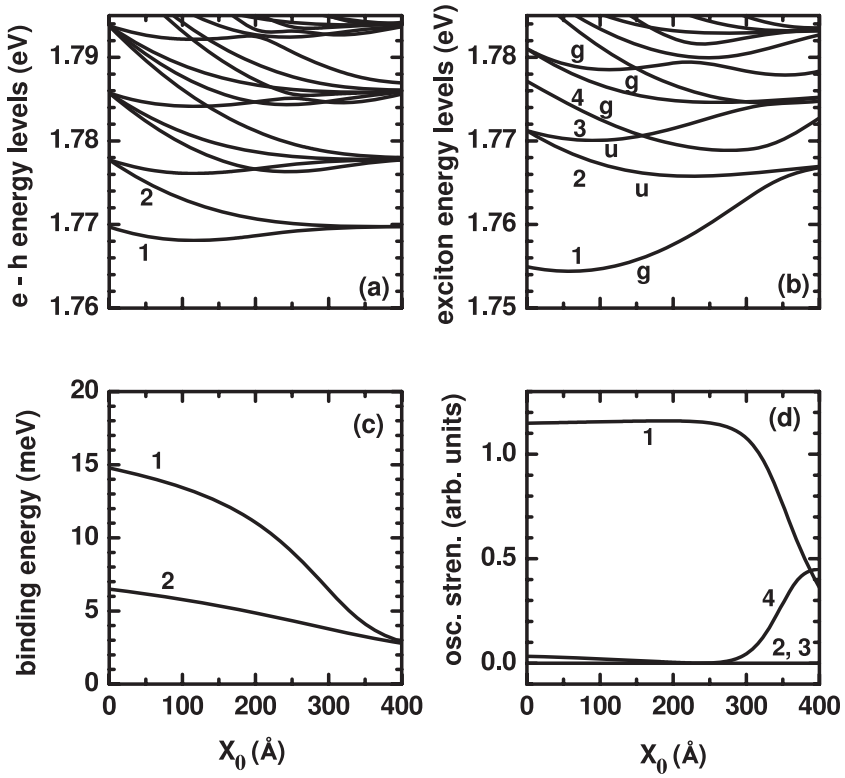

Figure 3. Results are as in figure 2, with $R = 150$ Å for the radius of each dot in the coupled system.

this range of energies for the in-plane confinement goes from 8 meV to 7 meV. These results are in agreement with the zero and infinite limits of X_0 for the lowest e–h energy levels in figures 2(a) and 3(a). The above results illustrate the order of magnitude of the different confinements here considered. In the $X_0 = 0$ limit, the excitons are dark, except those with $m = 0$. When X_0 increases, the excitons with odd angular moment remain dark because, in the present model, the lateral confinement potential only mixes states with the same parity. The variation of the oscillator strength (with light polarized in the x–y plane) as a function of the distance between the two coupled dots is shown in figures 2(d) and 3(d) for the first four exciton peak energies.

We turn now to figure 4 which illustrates how one may model the PL measurements reported by Yamagiwa *et al* [7] in laterally aligned GaAs QD pairs. For a quantum-well z confinement associated with $L = 52$ Å, an inter-dot distance $2X_0 = 450$ Å and a QD radius of ≈ 100 Å, the calculated result for the ground-state excitonic transition is in good agreement with the first observed structure at 1623 meV in the PL measurements (see figure 2(b) by Yamagiwa *et al* [7]). However, for these structural dimensions the dots are essentially uncoupled and the first-excited excitonic state is at about the same energy as the ground-state one. By considering the dot radii as 130 Å and $X_0 = 225$ Å, the two dots become coupled and the energies associated with the two excitonic energy transitions are in agreement with the experimental [7] PL features at 1623 and 1629 meV, provided a z quantum-well $L = 47$ Å confinement is considered (see calculated open dots in figure 4). In order to illustrate the

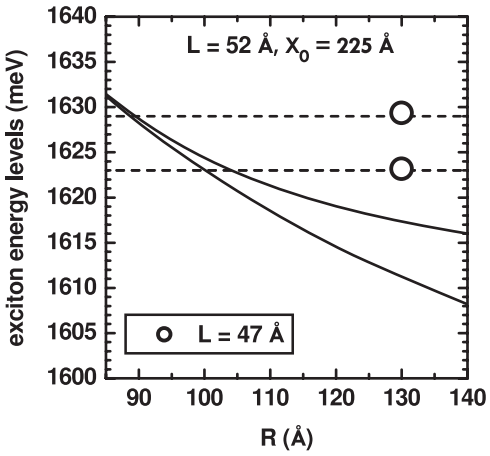

Figure 4. Exciton energy transition for a laterally coupled GaAs–$Ga_{0.73}Al_{0.27}As$ double quantum dot as a function of the radius of each dot. Full curves are the theoretical calculations with $X_0 = 225$ Å and a $L = 52$ Å quantum-well confinement in order to fit the lowest experimental data from Yamagiwa *et al* [7] (shown as the dashed line at 1623 meV). Open symbols are theoretical findings using $R = 130$ Å and a quantum-well width of 47 Å which fit the experimental data by Yamagiwa *et al* [7] (dashed lines at 1623 and 1629 meV).

dependence of the exciton states on the structural dimensions of the two-dot system, figure 5 displays the ground-state and first few excited correlated e–h energy transitions as functions of the distance ($2X_0$) between the two QDs, the R radius of each QD and the L quantum-well confinement of

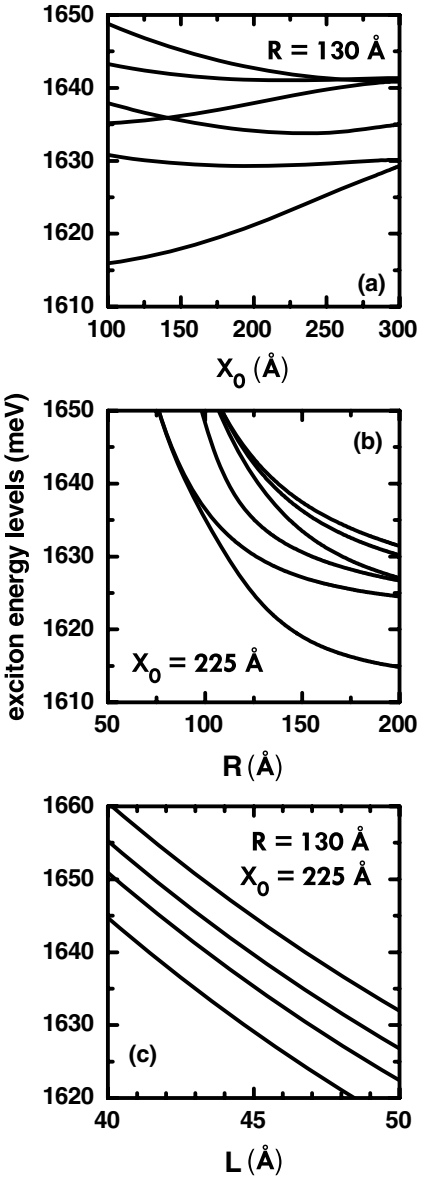

Figure 5. Exciton energy transitions for a laterally coupled GaAs–$Ga_{0.73}Al_{0.27}As$ double quantum dot, with a z-direction quantum-well width of 47 Å, as a function of half of the distance between the centers of the two dots (a) and of the radius of each quantum dot (b). Results in (c) are as functions of the z-direction quantum-well width used in the calculations.

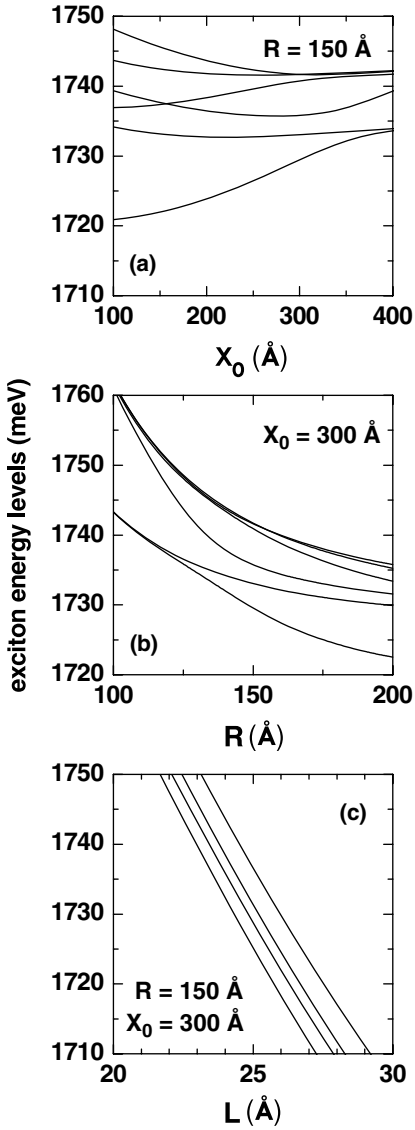

Figure 6. Results are as in figure 5 for a laterally coupled GaAs–$Ga_{0.7}Al_{0.3}As$ double quantum dot, with a z-direction quantum-well width of 24 Å in cases (a) and (b), whereas (c) shows calculations as functions of the z-direction quantum-well width.

the coupled pair of QDs. It is worthwhile mentioning that the structural dimensions used here to fit the experimental results, i.e. inter-dot distance $2X_0 = 450$ Å, QD diameter of 260 Å and QD height corresponding to $L \approx 50$ Å, are in qualitative agreement with atomic force measurements estimated by Yamagiwa *et al* [7] of 390 Å (±20 Å), 450 Å (±30 Å) and 100 Å (±20 Å), respectively. In the same way, one may attempt to guess the dimensions of a model two-dot structure which would reproduce the 1729.31 and 1733.49 meV PL peak measurements in figure 3 of the report by Kolb and Drew [8] in naturally occurring coupled GaAs QDs in narrow GaAs–$Ga_{0.7}Al_{0.3}As$ quantum wells, and one finds that a coupled pair of QDs with structural dimensions corresponding to $2X_0 = 600$ Å, QD diameter of 300 Å and QD height corresponding to a confinement in the z direction by a $L = 24$ Å quantum well, would fit the observed [8] ground state and first-excited excitonic states. Again, to illustrate the dependence of the exciton states on the structural dimensions of this model coupled QD system, figure 6 presents calculated results for the exciton energy transitions in laterally coupled GaAs–$Ga_{0.7}Al_{0.3}As$ double QDs as functions of the separation $2X_0$ between the centers of the two dots, the radius of each dot and the quantum-well width L associated with the z-direction confinement.

Finally, we have considered the effects of an applied magnetic field in the growth z direction of the laterally coupled QD heterostructure, in the case of the two model QD structures mentioned above, with dimensions such as to fit the first two PL exciton peaks (at zero magnetic fields) in the

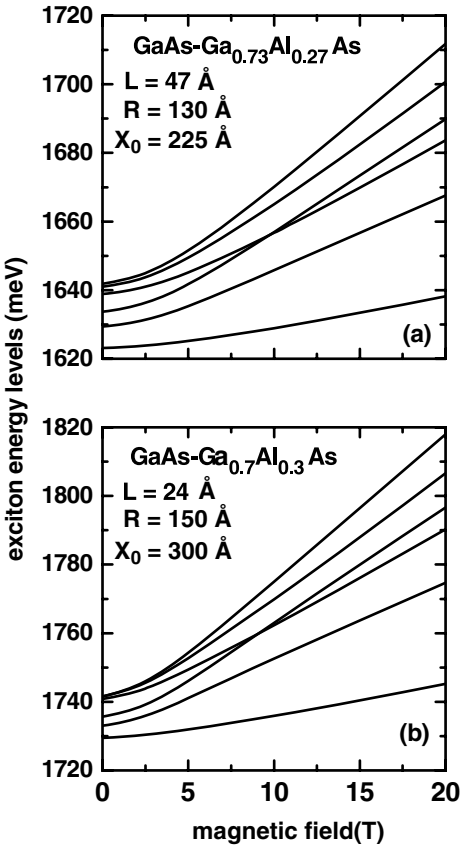

Figure 7. Exciton energy transition for a laterally coupled GaAs–$Ga_{1-x}Al_xAs$ double quantum dot as a function of the in-growth-direction-applied magnetic field. Dimensions of the double-dot structures have been taken (see text) such as to fit the first two PL exciton peaks (at zero magnetic fields) in the experiments by Yamagiwa *et al* [7] (a) and Kolb and Drew [8] (b).

experiments by Yamagiwa *et al* [7] and Kolb and Drew [8]. Calculated results for the exciton energy transitions in laterally coupled GaAs–$Ga_{1-x}Al_xAs$ double QDs as functions of the growth-direction-applied magnetic field are then presented in figure 7. As expected, one notes that a growth-direction-applied magnetic field leads to a blueshift of the correlated e–h transitions. An applied magnetic field corresponds to an additional confinement on the carriers, and one notes (cf figure 7) that 15 T is enough to remove the effects of geometrical confinement associated with the double QD system. The linear behavior of the ground and first few excited excitonic transitions, for magnetic fields larger than 15 T, is a clear signature of magnetic field (non-geometrical) confinement effects.

4. Conclusions

Summing up, we have performed a thorough theoretical study of the electronic and optical properties of laterally coupled double QD heterostructures under applied magnetic fields perpendicular to the plane of the dots. The excitonic states were obtained by using an expansion of the exciton envelope wavefunctions in terms of products of hole and electron quantum-well states with appropriate Gaussian functions for the various excitonic states, with calculations performed by using an extended variational approach in the effective-mass approximation. Calculations were shown to lead to the appropriate limits of one single QD, when the distance between the dots is zero, and of two uncoupled QDs, when the distance between the dots is large enough. Recent PL measurements in self-assembled laterally aligned GaAs QD pairs by Yamagiwa *et al* [7] and naturally/accidentally occurring coupled QDs in GaAs/GaAlAs quantum wells by Kolb and Drew [8] were modeled by realistic coupled double-dot structures, and the effects of growth-direction-applied magnetic fields on the magnetoexciton energy transitions were calculated for such systems. One should mention that the present calculated magnetoexciton results may be of importance when analyzing experimental measurements in laterally coupled double-dot heterostructures under growth-direction-applied magnetic fields.

Acknowledgments

This research was partially supported by the Colombian agencies COLCIENCIAS, CODI-Universidad de Antioquia, Facultad de Ciencias Exactas y Naturales-Universidad de Antioquia (CAD-exclusive dedication project) and the Excellence Center for Novel Materials/ COLCIENCIAS (contract no. 043-2005), the Chilean agencies CONICYT/Programa Bicentenario de Ciencia y Tecnología (CENAVA, grant ACT27), Fondecyt (grant nos. 1061237 and 7080147) and Universidad Técnica Federico Santa Maria (internal grant) and the Brazilian agencies CNPq, FAPESP and FAPERJ.

References

[1] Ortner G, Bayer M, Larionov A, Timofeev V B, Forchel A, Lyanda-Geller Y B, Reinecke T L, Hawrylak P, Fafard S and Wasilewski Z 2003 *Phys. Rev. Lett.* **90** 086404
[2] Krenner H J, Sabathil M, Clark E C, Kress A, Schuh D, Bichler M, Abstreiter G and Finley J J 2005 *Phys. Rev. Lett.* **94** 057402
[3] Neogi A, Morkocü H, Kuroda T, Tackeuchi A, Kawazoe T and Ohtsu M 2005 *Nano Lett.* **5** 213
[4] Schmidt O G, Deneke C, Kiravittaya S, Songmuang R, Heidemeyer H, Nakamura Y, Zapf-Gottwick R, Müller C and Jin-Phillipp N Y 2002 *IEEE J. Sel. Top. Quantum Electron.* **8** 1025
[5] Songmuang R, Kiravittaya S and Schmidt O G 2003 *Appl. Phys. Lett.* **82** 2892
[6] Beirne G J, Hermannstädter C, Wang L, Rastelli A, Schmidt O G and Michler P 2006 *Phys. Rev. Lett.* **96** 137401
[7] Yamagiwa M, Mano T, Kuroda T, Tateno T, Sakoda K, Kido G, Koguchi N and Minami F 2006 *Appl. Phys. Lett.* **89** 113115
[8] Kolb P W and Drew H D 2008 *Physica* E **40** 594
[9] Pacheco M, Barticevic Z and Claro F 1993 *J. Phys.: Condens. Matter* **5** A363
Pacheco M, Barticevic Z and Claro F 1995 *Phys. Rev.* B **51** 14414
Pacheco M and Barticevic Z 1997 *Phys. Rev.* B **55** 10688
Pacheco M and Barticevic Z 1999 *J. Phys.: Condens. Matter* **11** 1079

[10] Barticevic Z, Pacheco M, Duque C A and Oliveira L E 2003 *Phys. Rev.* B **68** 073312
Duque C A, Porras-Montenegro N, Barticevic Z, Pacheco M and Oliveira L E 2006 *J. Phys.: Condens. Matter* **18** 1877
Barticevic Z, Pacheco M, Duque C A and Oliveira L E 2007 *J. Phys.: Condens. Matter* **19** 216224
Barticevic Z, Pacheco M, Duque C A and Oliveira L E 2007 *Eur. Phys. J.* B **56** 303
[11] Li E H 2000 *Physica* E **5** 215